

Demonstration for rearrangeable nonblocking 8×8 matrix optical switches based on extended banyan networks

De-Gui Sun^{1,3*}, Ying Zha^{2,3}, Tiegeng Liu², Ying Zhang³, Xiaoqi Li³, and Xiuhua Fu¹

1) School of Optoelectrical Engineering, Changchun University of Science and Technology

7089 Weixing Road, Changchun, JL 130022, China

2) Key Laboratory of Opto-Electronics Information and Technical Science of Ministry of Education, School of Precision Instrument and Opto-electronics Engineering, Tianjin University, Tianjin 300072, China

3) State Key Laboratory of Applied Optics, Changchun Institute of Optics, Fine Mechanics and Physics Chinese Academy of Sciences □ 16 East Nanhua Street, Changchun, JL 130031, China

* deguisun_b@yahoo.com

Abstract: Based on the CROSSBAR network (CN) and the BANYAN network (BN), two new rearrangeable nonblocking constructions of extended BANYAN network (EBN) were proposed for implementing 8×8 optical matrix switch. The interconnection characteristics of these two types of rearrangeable nonblocking EBN were studied, and the logic program for driving switching units was provided. The calculated insertion loss is 3.3 dB for 8×8 optical matrix switch. Silica waveguide 8×8 matrix optical switch was designed and fabricated according to the calculated results. The silica waveguide propagation loss of 0.1dB/cm and waveguide-fiber coupling loss of 0.5dB/point were measured. With the fabricated 8×8 matrix optical switch, optical insertion loss of 4.6 dB, cross-talk of -38 dB, polarization dependent loss of 0.4 dB, averaged switching power of 1.6 W, and switching time of 1 ms were obtained. A basic agreement between experimental results and theoretical calculated values was achieved.

©2007 Optical Society of America

OCIS codes: (130.3120) Integrated optics devices; (060.1810) Couplers, switches, and multiplexers; (230.7390) Waveguides, planar circuits.

References and links

1. X. K. Sun and J. J. Zhang, *Fiber Communication Technology*, S. P. Wang, ed. (Academic, Beijing, 2001) pp. 317-318.
2. X. M. Chen and P. Zhou, "Optical switch mainstream technologies," *Opt. Commun. Technol.* **30**(3), 53-55 (2006).
3. D. G. Sun, Z. Liu, Y. Zha, W. Deng, Y. Zhang, and X. Li, "Thermo-optic waveguide digital optical switch using symmetrically coupled gratings," *Opt. Express* **13**(14), 5463-5471 (2005).
4. D. G. Sun, W. Deng, S. E. Y. Zha, Z. Liu, X. Li, "Study for performance of the thermo-optic matrix switches with flexible switching units and Banyan networks," *Opt. Eng.* **45**(1), 014602(2006).
5. W. D. Ma, Q. Liu, and G. H. Hu, "Planar lightwave circuit technology and practical part," *Fiber Commun. Technol.* **7**, 27-28 (2003).
6. G. I. Papadimitriou, C. Papazoglou, and A. S. Pomports, "Optical switching: switch fabrics, techniques, and architectures," *J. Lightwave Technol.* **21**(2), 384-405 (2003).
7. R. Ramaswami and K. N. Sivarajan, *Optical Networks: A Practical Perspective*, J. Mann, Y. Overton, C. Palmer and K. Johnson, eds. (Academic, San Francisco, Calif., 1998) pp. 329-389.
8. G. B. Adams and H. J. Sigel, "The extra stage cube: A fault tolerant interconnection network for supersystems," *IEEE Trans. Computers* **31**(5), 443-445 (1982).
9. C. S. Raghavendra and A. Varma, "Fault-tolerant multiprocessors with redundant path interconnection networks," *IEEE Trans. Computers* **35**(4), 307-316 (1986).
10. N. F. Tzeng, P. C. Yew, and C. Q. Zhu, "A fault-tolerant scheme for multistage interconnection networks," *Parallel Processing, Proc. Int'l Conf.*(1), 368-375 (1985).

11. V. P. Kumar and S. M. Reddy, "Augmented shuffle-exchange multistage interconnection networks," *IEEE Trans. Computers* **20**(6), 30-40 (1987).
 12. M. P. Eamshaw, J. B. D. Soole, M. Cappuzzo, *et al.*, "8×8 optical switch matrix using generalized Mach-Zehnder interferometers," *IEEE Photon. Lett.* **15**(6), 810-812 (2003).
-

1. Introduction

Two essential modules in full-optical network are optical cross connect (OXC) and optical add/drop multiplexing (OADM), and matrix optical switch is the central part of an OXC system. The exploitation of large-scale matrix optical switches is the practical demand in the modern optical communications and information processing systems [1-3]. Matrix optical switch is a device to realize the switching operations of optical signals among multiple channels, so it is required to connect optical signals between any input and output ports without blocking. According to the blocking possibility, an optical matrix switch can be categorized into strictly nonblocking and rearrangeable nonblocking [4]. If a connection can be built between any available pair of input-output ports without changing any existing connections, it is strictly nonblocking. If all the input-output connections can be built by rearranging the built connections, it is called rearrangeable. Planar lightwave circuit (PLC) technologies can radically overcome the limitation of conventional mechanical technologies and micro-electro-mechanical system (MEMS) technologies in switching speed and operating stability because of its no-moving-part property. Silica-on-silicon waveguide technology is widely investigated in fabricating large-scale optical matrix switch because of its particular merits such as low optical loss, excellent compatibility with mature semiconductor technologies, high coupling efficiency with fiber, and low cost [4-5].

In fact, a PLC-based nonblocking large-scale optical matrix switch is an effective combination of a network of optical signal links and a permutation of switching units. Since the Mach-Zehnder interferometer (MZI) structure switches are the most suitable for silica waveguides, the networks based on the 2×2/1×2 switches are preferred to implement the silica-PLC-based large-scale optical matrix switches [4-6]. A CROSSBAR network (CN) is a typical strictly non-blocking optical switch network, and is widely used in integrated optical components [6-7], especially in large-scale nonblocking matrix optical switches. However, many interconnection stages and switching units of CROSSBAR network for a switching operation result in larger device size and more optical loss, and further restrict its application in matrix optical switches based on PLC technology. A BANYAN network (BN) with butterfly interconnection construction needs fewer switching units and interconnection stages, so it has a smaller device dimension and a lower loss than a CROSSBAR network for the same scale of matrix switches. Thus, the BN also attracts more attention for constructing large-scale nonblocking optical switch recently. A BANYAN network is, however, an inner blocking network, because two optical signals from different input ports to different output ports sometimes pass through the same switching units synchronously, and then they are probably blocked each other. To solve this problem, some nonblocking networks are altered by combining different trimmed networks or adding inside linking [8-11], but their much more interconnection stages and links result in a large network or a complicated routing process, so that approach is not a good choice from the view point of fabrication.

In this paper, we analyzed the construction characteristics of CN and BN in detail, and compared the optical insertion losses between CN- and BN-based matrix optical switches. Then, we define an extended BANYAN network (EBN), which is made up of the basic BANYAN network. The EBN is not a strictly nonblocking network, but it can implement nonblocking switching operations by pre-optimizing the signal routes with a given drive program, so the EBN-based switch is rearrangeable nonblocking. The rearrangeable nonblocking property of an 8×8 optical switch with EBN construction and the logic diagram for driving switching units were provided and analyzed, and the interconnection optical loss

and the averaged switching power were calculated. Based on the EBN construction, we fabricated a silica waveguide 8×8 optical matrix switch and obtained expectable experimental results. Accordingly, the experiments prove that this type of extended BANYAN networks shows some inherent advantages in aspects of device size and optical loss over other constructions.

2. Network construction analysis

2.1 Construction analysis of CROSSBAR and BANYAN network

Figure 1 (a) and Fig. 1(b) are the constructions based on CN and BN with $N=8$, respectively. As shown in Fig. 1(a), for a matrix optical switch of CN construction with a scale of N , the numbers of linking stages, switching units stages and total switching units are $n_{cs} = N - 1$, N and N^2 , respectively. A signal need pass through n_{cc} stages of switching units from an input to an output, where $n_{cc} = 2m - 1$ ($m = 1, 2, \dots, N$). As a result, it brings about the big device size, large optical loss, and the non-uniformity of the signal paths. Thus, some additional switching units are used for the purpose of compensating the non-uniformity of optical loss [12], and make all signal paths have $2N - 1$ stages of switching units. As shown in Fig. 1(b), for an $N \times N$ matrix optical switch based on the BN construction with butterfly interconnection, the numbers of intersectional linking stages, switching units stages and total switching units are n_{bs} , n_{bc} and $N \cdot n_{bc}$, respectively, where $n_{bs} = \log_2^N$ and $n_{bc} = \log_2^N + 1$. All the signals between any input port and output port will track $\log_2^N + 1$ switching units. With the increasing of N , the superiority of BN is more apparent in the aspects of device size and optical loss for large-scale matrix optical switches.

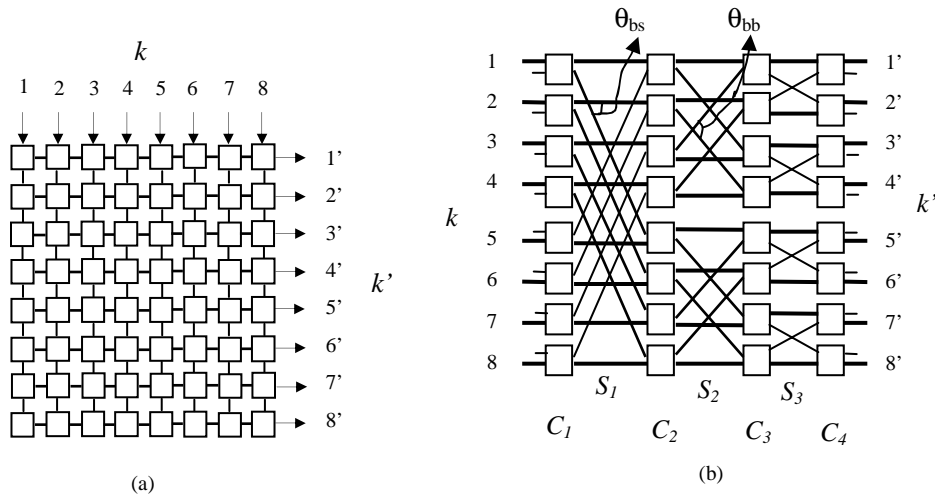


Fig. 1. Constructions of the CROSSBAR network and the BANYAN network with the width of $N=8$: (a) is the CROSSBAR network; (b) is the BANYAN network

In the MASK design, we avoid the scenario of three-waveguide intersection, namely two butterfly lines and a horizontal line intersect one another at a crossing point, by designing the proper layout of linking waveguides. Therefore, there are only two scenarios of intersections. One is the intersection between a horizontal line and a butterfly line with the intersecting angle of θ_{bs} , and the other is the intersection between two butterfly lines with the intersecting angle of θ_{bb} . It is easy to find $\theta_{bs} = \theta_{bb} / 2$. Corresponding to the above two types of

intersections, two intersection-induced losses of $L_{\text{inter}}(\theta_{bs})$ and $L_{\text{inter}}(\theta_{bb})$ are defined. It is easy to see from Fig. 1(b) that each butterfly line intersects with the $N/2^i$ reverse butterfly lines, and intersects with the $N/2^i - 1$ horizontal lines. The intersection numbers of these two types of intersections are defined as $n_{\text{inter}}(\theta_{bb})$ and $n_{\text{inter}}(\theta_{bs})$, respectively, and given by

$$n_{\text{inter}}(\theta_{bb}) = N/2^i \quad i = 1, 2, \dots, n \quad (1a)$$

$$n_{\text{inter}}(\theta_{bs}) = N/2^i - 1 \quad i = 1, 2, \dots, n \quad (1b)$$

Then the total intersection loss is

$$TL_{\text{inter}} = \sum_{i=1}^n L(\theta_{bb}) \cdot n_{\text{inter}}(\theta_{bb}) + \sum_{i=1}^n L(\theta_{bs}) \cdot n_{\text{inter}}(\theta_{bs}) \quad (2)$$

Where, $L(\theta_{bb})$ and $L(\theta_{bs})$ are the corresponding intersection-induced losses at the intersection angle of θ_{bb} and θ_{bs} , respectively. If an individual MZI unit loss is L_{MZI} , the number of MZI units for an optical signal to pass through is n_{MZI} , the averaged MZI length is l_{MZI} , and waveguide propagation loss is L_{prop} , the total loss of switching units and the total propagation loss can be calculated by

$$TL_{\text{switch}} = n_{\text{MZI}} L_{\text{MZI}} \quad (3)$$

$$TL_{\text{prop}} = n_{\text{MZI}} l_{\text{MZI}} L_{\text{prop}} \quad (4)$$

Considering the fiber-waveguide coupling loss L_{WFC} , finally, we obtain the insertion loss IL of the matrix optical switch of BANYAN network as

$$IL = TL_{\text{inter}} + TL_{\text{switch}} + TL_{\text{prop}} + 2L_{\text{WFC}} \quad (5)$$

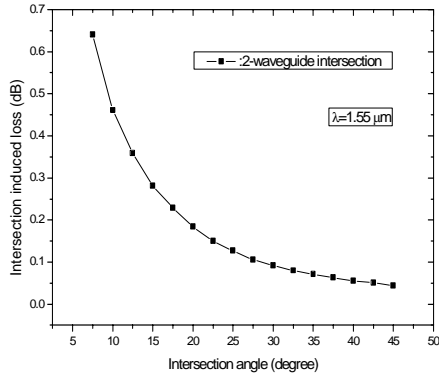


Fig. 2. Simulation results of the intersection-induced optical loss versus the intersection angle

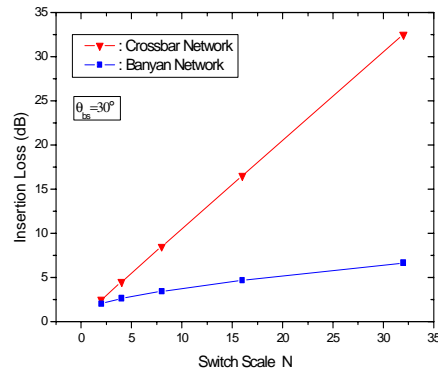


Fig. 3. Simulation results of the insertion optical loss versus the switch scale N

With the simulation software tool OptiBPM, we simulate the influence of intersection angle on intersection-induced loss with respect to two-waveguide intersecting as shown in Fig. 2. Note that, the intersection-induced optical loss quickly decreases with angle increasing, specially $L_{\text{inter}}(\theta_{bs})$ is 0.09dB and $L_{\text{inter}}(\theta_{bb})$ is less than 0.01dB when angle θ_{bs} is 30 degree. According to the design and measured results, we take the averaged length

of each individual switching unit as 1.0cm , the propagation loss 0.1dB/cm , the fiber-waveguide coupling loss 0.5dB/point , and the access loss of switching unit 0.4dB . With Eqs. (1) to (5), the relations of insertion loss IL versus the switch width N of the BN and the CN are obtained as shown in Fig. 3. The great superiority of the optical matrix switch based on the BN construction can be seen in optical loss and device size when N is large.

To study the networks from topology, the CROSSBAR network is strictly nonblocking network, and any connection can be established between an available input-output pair irrespective of the operating state of the network. Nevertheless, the BANYAN network is inner blocking construction, and its established connections maybe impact the building of a new connection. The reason is that there is only one possible path for each optical signal to track from an input port to an output port, and when two optical signals from different input ports to different output ports track the same switching unit, blocking will appear. Therefore, some extra-steps should be added to solve this problem. For instance, as shown in Fig. 1(b), the two signals from input ports 1 and 5 to output ports 1' and 2' will be blocked each other at the switching unit 1 of stage C_2 , and also the signals from input ports 1 and 5 to output ports 3' and 4' will be blocked each other at the switching unit 2 of stage C_2 . In general, when two optical signals input from the ports with different number of 4, i.e. from input ports 1 and 5, or from ports 2 and 6, or from ports 3 and 7, or from ports 4 and 8, and to the output of the following four groups of ports, i.e. the output of ports 1' and 2', or of ports 3' and 4', or of ports 5' and 6', or of ports 7' and 8', they will be blocked at the switching units of stage C_2 . In other cases, the optical signals can pass through the BN and reach the destination output ports without blocking.

2.2 Construction analysis of extended BANYAN network

Figure 4(a) and Fig. 4(b) show the type-I and type-II EBN constructions of 8×8 optical switch, respectively. In them, each small square is a switching unit with MZI construction. The two types of EBN constructions are both formed by extending a stage in horizontal direction, which has the same forms as the stages of the BN construction. The extended stage of type-I construction has the same form as stage S_2 of the BN construction, but that of type-II construction has the form of stage S_1 instead of stage S_2 . So, each of the two types of extended networks has five stages and total forty switching units. With each of the EBN constructions, two optional paths can be chosen for an optical signal to track in each input-output pair. Accordingly, we can properly choose the signal path from the two possible paths to realize rearrangeable nonblocking signal routing.

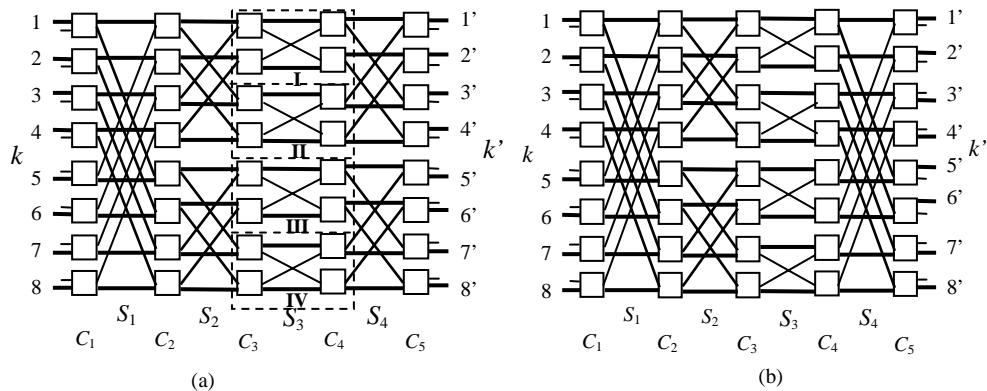


Fig. 4. Constructions of the two types of extended BANYAN network: (a) the type-I construction; (b) the type-II construction

The signal routing process of type-I construction is illustrated in detail as follows. As shown in Fig. 4(a), stage S_2 is divided into two groups, and stage S_3 is divided into four groups of I to IV frames, marked with dashed line. Here, only upper I and II groups of stage S_3 is considered. If two signals, coming from ports k and $k+4$ ($k=1,2,3,4$) of stage C_1 and go to the destination output ports k' and $k'+1$ ($k'=1',3'$) of stage C_5 , pass through I and II groups separately, the blocking will be avoided. To simplify the logic diagram, we define that the signals coming from ports $1'$ and $3'$ fixedly pass through I and II groups, respectively. In the general case, the signals coming from the ports $2'$ and $4'$ also pass through I and II groups, respectively, but the possible case of blocking can be avoided by exchanging the two signals' paths to II and I groups, respectively. In the same manner, the signals from ports $5'$ to $8'$ yield to the same case as the signals from ports $1'$ to $4'$.

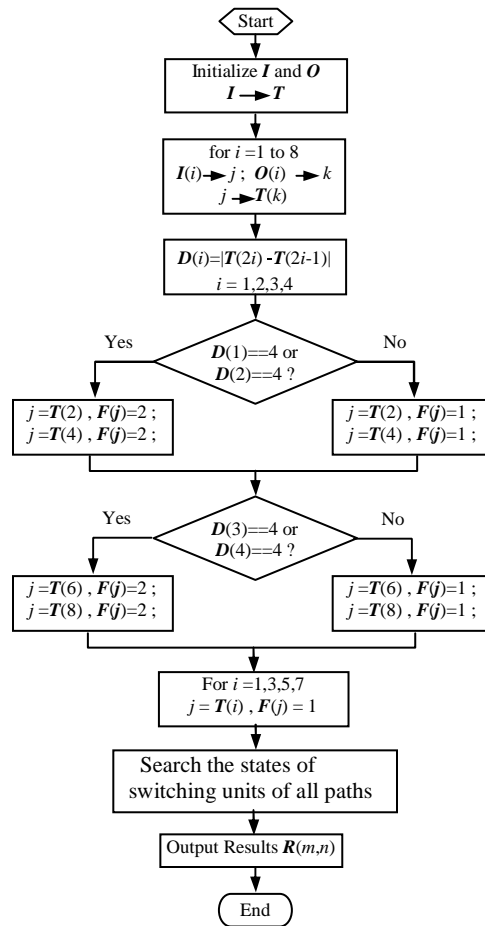


Fig. 5. Flow diagram of the switching driver with respect to the type-I extended BANYAN network

Several vectors are defined in order to address the electrical-driven switching units with a program. The vectors $I(1 \times 8)$ and $O(1 \times 8)$ are respectively the numbers of input ports and output ports, and $M(1 \times 4)$ is the number difference of the input ports of the signals which are for two adjacent output ports, where $M(i) = |I(2i) - I(2i-1)|$ ($i=1,2,3,4$). Vector $F(1 \times 8)$ is defined to mark the signal path according to the signal output choice at the switching units of stage

C_4 , and is set as 1 for straight line output and 2 for butterfly intersectional line output. $R(8 \times 5)$ is the matrix for operating the switching units, and $R(m,n)$ is defined to stand for the value of switching units, and the value of $R(m,n)$ is 1 when the switching unit of the m -th row and the n -th column should be activated electrically, otherwise its value is 0. Based on the previous depiction about nonblocking property of the signal routes, matrix R can be obtained by the flow diagram as shown in Fig. 5, where T is the temporary vector, and i, j, k are temporary variables for the program operations.

For the type-II construction, the signals coming from 1' to 4' and from 5' to 8' should yield to the routes in the upper group and the lower group of stage C_2 , respectively. When a blocking state occurs, the signals arriving at ports k' and $(k'+4)$ ($k'=2$ or 4) should be exchanged to the routes in the lower group and the upper group of stage C_2 , respectively. The flow diagram of the type-II construction is not described again because of its similarity with that of the type-I. In the signal routing program, we can define a state list to memorize the switching units on/off states of the accessible routes of all input-output pairs. Based on the previous process for finding the signal route, the switching matrix T will be produced. Further more, we can create the drive signals to perform the switching actions with a drive circuit. As an illustration, we completed a calculation program of matrix T with the flow diagram as shown in Fig. 5 and obtained partial results. Table 1 lists eight groups of the values of the vector F and the matrix T with different switching states. According to the values, we can judge the optical paths of all the signals and the activities of all the switching units. For instance, as shown in the table 1, the V -th group provides the rearranged optical paths and the switching units activities when possible blockings exist. When the input-output-port pairs of optical signals are 1-1', 2-3', 3-5', 4-7', 5-2', 6-4', 7-6', and 8-8', the optical paths of signals 5-2', 6-4', 7-6', and 8-8' are reelected by passing through groups II, I, IV, and III at stage S_3 in the frames of Fig. 4(a), respectively. Thus, each optical signal can find a path without blocking each other to pass through from input ports to output ports.

Table 1. Calculation results of matrix T according to type-I EBN construction

I							II							III									
In-Out	T					F	In-Out	T					F	In-Out	T					F			
	C ₁	C ₂	C ₃	C ₄	C ₅			C ₁	C ₂	C ₃	C ₄	C ₅			C ₁	C ₂	C ₃	C ₄	C ₅				
1-1'	1	1	1	1	1	1	1-8'	0	1	1	0	1	1	1	1	1	1	1	1	1	1	1	1
2-2'	1	1	0	0	1	1	2-7'	0	1	0	1	1	1	1	2-5'	0	0	0	1	1	1	1	1
3-3'	1	0	0	0	0	1	3-6'	0	0	0	1	0	1	1	3-2'	1	1	1	0	0	0	1	1
4-4'	1	0	1	1	0	1	4-5'	0	0	1	0	0	1	1	4-6'	0	0	0	0	0	0	1	1
5-5'	1	0	1	1	0	1	5-4'	0	0	1	0	0	1	1	5-3'	0	0	0	0	0	0	1	1
6-6'	1	0	0	0	0	1	6-3'	0	0	0	1	0	1	1	6-7'	1	1	1	0	0	0	1	1
7-7'	1	1	0	0	1	1	7-2'	0	1	0	1	1	1	1	7-4'	0	0	0	1	1	1	1	1
8-8'	1	1	1	1	1	1	8-1'	0	1	1	0	1	1	1	8-8'	1	1	1	1	1	1	1	1
IV							V							VI									
In-Out	T					F	In-Out	T					F	In-Out	T					F			
	C ₁	C ₂	C ₃	C ₄	C ₅			C ₁	C ₂	C ₃	C ₄	C ₅			C ₁	C ₂	C ₃	C ₄	C ₅				
1-5'	0	0	1	0	1	1	1-1'	1	1	1	1	1	1	1	1-1'	1	1	1	1	1	1	1	1
2-1'	1	1	1	0	0	1	2-3'	1	0	0	1	0	1	1	2-3'	1	0	1	0	1	1	1	1
3-3'	1	0	0	0	0	1	3-5'	0	0	0	1	0	1	1	3-5'	0	1	1	1	0	1	1	1
4-7'	0	0	0	0	1	1	4-7'	0	0	1	1	1	1	1	4-7'	0	0	1	0	0	1	1	1
5-6'	1	1	1	1	0	2	5-2'	0	0	0	1	0	2	2	5-8'	1	1	0	1	0	1	1	1
6-2'	0	0	1	1	1	2	6-4'	0	0	1	1	1	2	2	6-6'	1	0	0	0	0	1	1	1
7-4'	0	0	0	1	1	2	7-6'	1	1	1	1	1	2	2	7-4'	0	1	0	1	1	1	1	1
8-8'	1	0	0	1	0	2	8-8'	1	0	0	1	0	2	2	8-2'	0	0	0	0	1	1	1	1

3. Theoretical calculation

With the previous analysis, the optical loss of the BN and EBN construction is compared. Figure 6(a) displays the proportion of different optical loss in the insertion loss. We can notice

that most of optical loss of EBN is from the access loss of switching units and intersection-induced loss, and the two types of EBN constructions have the same loss of switching units and propagation loss, but type-II construction has a larger intersection-induced optical loss than that of type-I construction. When N is small, the loss of switching units is larger than intersection-induced loss, but the intersection-induced loss increases faster than the loss of switching units with N , namely, the influence of intersection-induced optical loss on insertion loss becomes more serious. Figure 6(b) shows the simulation result of insertion loss versus switch width N . It is easy to see from Fig. 6(b) that two types of EBN constructions have larger insertion losses than BN construction and their difference in the insertion loss becomes larger with N , but the increasing speed of the type-I construction is less than that of the type-II construction. Comparing with that of the CN construction in Fig. 3, the insertion losses of EBN constructions are relatively smaller obviously.

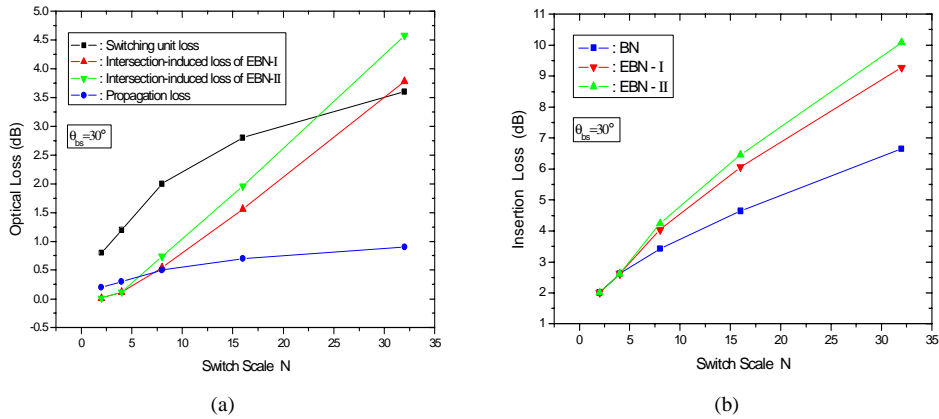


Fig. 6. Simulation results of optical losses versus switch scale N : (a) the optical losses of the EBN construction versus switch scale N ; (b) the insertion losses of the BN and EBN constructions versus switch scale N

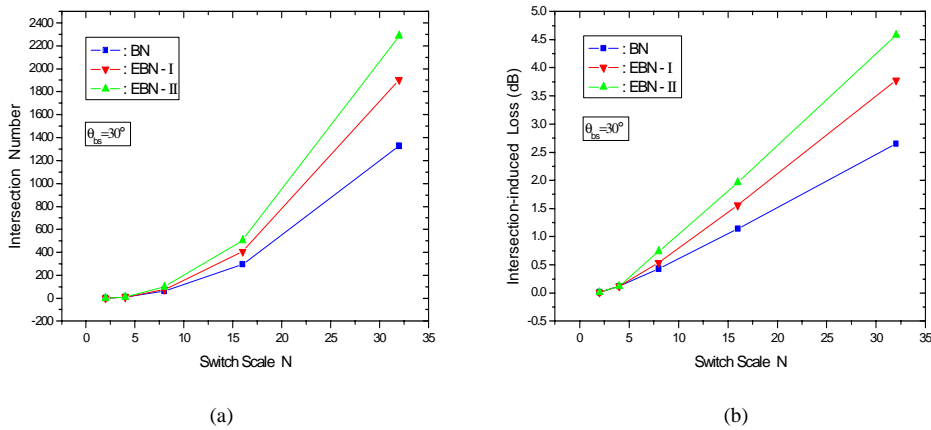


Fig. 7 Simulation results of the intersection number and intersection-induced loss versus the switch scale N : (a) the intersection number versus switch scale N ; (b) the total intersection-induced loss at $\theta_{bs} = 30$ degree

The relations of the intersection number and the intersection-induced loss versus switch width N are depicted in Fig. 7(a) and Fig. 7(b), respectively. It can be found from Fig. 7 that the two parameters increase more rapidly with N , and the two types of EBN constructions and BN construction have the similar changing trends, but that of the type-I are less than that of type-II construction at all time. The proportion of intersection-induced loss is much smaller and can be ignored when N is small, but its influence on insertion loss will be dominant and must be considered when N is big. Figure 8 shows the relations of the switching power of two types of EBN constructions with different N when all the N channels of signals operate synchronously. As for an 8×8 matrix optical switch, the total switching power of 10W and the averaged switching power of 1.2W/ch are calculated, and they are all relatively larger than the counterparts of CN construction.

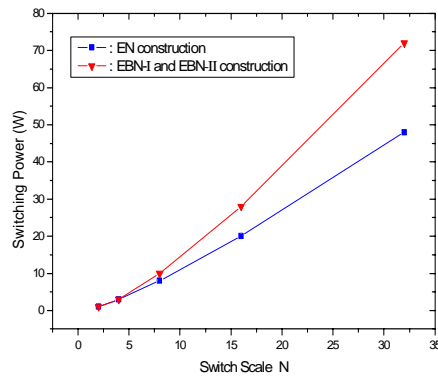


Fig. 8. Simulation results of the total switching power versus the switch width N

4. Experimental results and discussion

With the simulation results, we designed a rearrangeable nonblocking 8×8 matrix optical switch with the type-I EBN construction. The refractive index difference, the cross-sectional size, and the intersection angle of waveguides are 0.75%, $5.5 \times 5.5 \mu\text{m}^2$ and 30 degree, respectively.

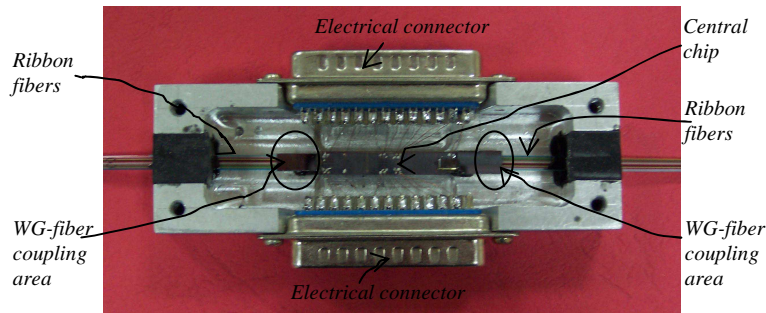


Fig. 9. Photo image of 8×8 matrix optical switch with the EBN construction and silica waveguides, where WG stands for waveguide

With the PEVCD deposition and RIE etching, we fabricated a sample of 8×8 matrix optical switch, and the photo image of a packaged device is depicted in Fig. 9, where the central chip, ribbon fibers, waveguide-fiber coupling areas and electrical connectors are labeled. Figure 10 shows the relations of optical output versus the applied electrical power with respect to the wavelengths of 1530, 1550 and 1570 nm, respectively. The measured

values of propagation loss and waveguide-fiber coupling loss were respectively 0.1dB/cm and 0.5dB/facet at 1550nm wavelength. Further several main parameters such as insertion loss (IL), cross-talk (XT), polarization dependent loss (PDL), switching power consumption (SPC), and switching time (ST) were obtained as listed in Table 2. The average measured values of these parameters are 4.6dB, -38dB, 0.4dB, 1.6W/ch, and 1.0ms, respectively. Note that the measured value of IL is closed to what is obtained in simulation, and as well the results of XT and ST are also excellent. In addition, the central-chip size is only $55\times 6\text{mm}^2$, which is much smaller than what is based on the CN, accordingly the insertion loss is also reduced a lot. It turns out that this type of extended BANYAN construction has promising applications for large-scale optical switches with low loss and low cost.

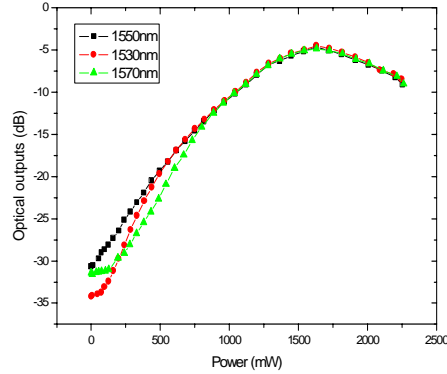


Fig. 10. Measured results of insertion loss versus applied power of the fabricated 8×8 optical switch with the EBN construction and silica waveguides

Table 2. Measured results of 8×8 optical matrix switch

Items	IL	XT	PDL	SPC	ST
Unit	dB	dB	dB	W/ch	ms
Value	4.6	-38	0.4	1.6	1

5. Conclusion

Two types of extended BANYAN networks with rearrangeable nonblocking character are proposed, and the main characteristics, including insertion loss and butterfly intersection, are analyzed. The blocking property and the signal routing process of an 8×8 matrix optical switch are discussed in detail. With a fabric of Silica-based 8×8 matrix optical switch of approximate 5.5cm in length, the measured insertion loss of 4.6dB is closed to the simulation result. It is proved that the extended BANYAN network is superior to the CROSSBAR network in size and optical loss because of its fewer stages of switching units. It is easy to finish 8×8 matrix optical switch in a $4''$ -wafer without looped layout design. It is necessary to remind that although no blocking of the EBN construction is made sure in theory and by the actual fabric, the further study of the general mathematic logic diagram of signal routing should be made to realize the application of this network in universal sense.

Acknowledgments

This work is co-supported by the 100-Person-Plan Foundation of Chinese Academy of Sciences and the R&D Foundation of Changchun University of Science and Technology.